# **Functional Flow Matching**

# Gavin Kerrigan

Department of Computer Science University of California, Irvine gavin.k@uci.edu

# Giosue Migliorini

Department of Statistics University of California, Irvine gmiglior@uci.edu

## **Padhraic Smyth**

Department of Computer Science University of California, Irvine smyth@ics.uci.edu

# **Abstract**

In this work, we propose Functional Flow Matching (FFM), a function-space generative model that generalizes the recently-introduced Flow Matching model to operate directly in infinite-dimensional spaces. Our approach works by first defining a path of probability measures that interpolates between a fixed Gaussian measure and the data distribution, followed by learning a vector field on the underlying space of functions that generates this path of measures. Our method does not rely on likelihoods or simulations, making it well-suited to the function space setting. We provide both a theoretical framework for building such models and an empirical evaluation of our techniques. We demonstrate through experiments on synthetic and real-world benchmarks that our proposed FFM method outperforms several recently proposed function-space generative models.

# 1 Introduction

Generative models have seen a meteoric rise in capabilities on various domains, such as images [Dhariwal and Nichol, 2021, Kang et al., 2023], video [Saharia et al., 2022, Ho et al., 2022], and audio [Kong et al., 2021, Goel et al., 2022]. Despite these recent successes, many methods implicitly assume that the data distribution of interest is supported on a finite-dimensional space. However, there are multiple important applications that involve data that is inherently infinite-dimensional. For instance, draws from a time series, solutions to partial differential equations, and audio signals are naturally represented as *functions*.

For functional data, the typical generative modeling approach is to operate directly on a discretization of this data [Tashiro et al., 2021, Rasul et al., 2021a, Yan et al., 2021]. However, these approaches are often tied to a chosen discretization, and such methods are often ill-posed in the limit of zero discretization error. To overcome these limitations, recent methods have proposed building generative models directly in function spaces. For instance, Kerrigan et al. [2023] and Lim et al. [2023a] propose function-space diffusion models, and Rahman et al. [2022] propose a function-space GAN.

In this work, we add to this growing literature on function-space generative models. In particular, we propose Functional Flow Matching (FFM), a continuous-time normalizing flow model for functional data. Given that Euclidean normalizing flow methods [Papamakarios et al., 2021, Kobyzev et al., 2020] are posed in terms of densities, which in general may not exist in infinite-dimensional spaces, a key challenge of performing this generalization is to pose a purely measure-theoretic flow based model. In particular, our model is a generalization of the recently proposed Flow Matching model of Lipman et al. [2023].

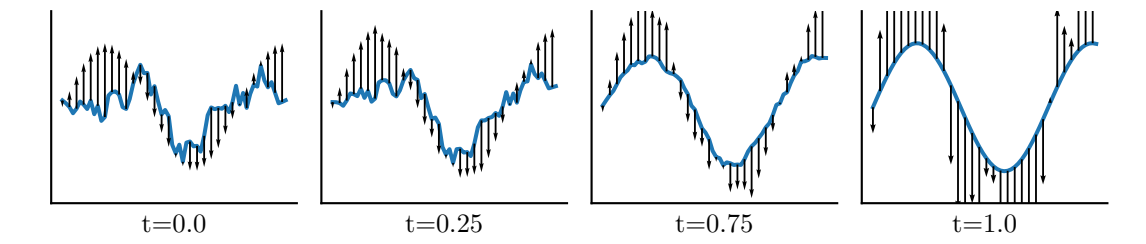


Figure 1: An illustration of our FFM method. The vector field  $v_t(f) \in \mathcal{F}$  (in black) transforms a noise sample  $g \sim \mu_0 = \mathcal{N}(0, C_0)$  drawn from a Gaussian process with a Matérn kernel (at t=0) to the function  $f(x) = \sin(x)$  (at t=1) via solving a function-space ODE. By sampling many such  $g \sim \mu_0$ , we define a conditional path of measures  $\mu_t^f$  approximately interpolating between  $\mathcal{N}(0, C_0)$  and the function f, which we marginalize over samples  $f \sim \nu$  from the data distribution in order to obtain a path of measures approximately interpolating between  $\mu_0$  and  $\nu$ .

Our proposed FFM model operates by first constructing a path of conditional Gaussian measures, approximately interpolating between a fixed reference Gaussian measure and a given function. A path of measures interpolating between said reference measure and the data distribution is obtained by marginalizing these conditional paths over the data distribution. We then learn a vector field on our space of functions which approximately generates this path of measures, allowing us to generate samples from our data distribution by solving a differential equation parametrized by this vector field. See Figure 1 for an illustration of our approach.

A key benefit of our approach is that it allows for simulation-free training, in the sense that no samples are drawn from the model during training. Moreover, our training objective is a regression objective, allowing us to avoid difficulties with regards to maximum likelihood training in a functional setting. We empirically verify our framework on a well-known functional datasets, and we demonstrate that the FFM model is able to outperform several recently proposed function-space generative models in terms of various statistics on an unconditional generation task. In addition, we propose several methods for performing conditional generation with the FFM model.

# 2 Related Work

Flow Matching and Normalizing Flows. We generalize the Flow Matching model of Lipman et al. [2023], which is a novel approach to simulation-free continuous-time normalizing flows [Chen et al., 2018, Papamakarios et al., 2021, Kobyzev et al., 2020] that has demonstrated impressive capabilities on several image generation tasks. However, Flow Matching and other recently proposed simulation-free continuous normalizing flows have only been explored for data distributions supported on finite-dimensional spaces, such as Euclidean spaces [Lipman et al., 2023, Albergo and Vanden-Eijnden, 2023, Liu et al., 2022, Neklyudov et al., 2022] and Riemannian manifolds [Chen and Lipman, 2023, Ben-Hamu et al., 2022]. In contrast, we propose Functional Flow Matching, a continuous-time normalizing flow for infinite-dimensional data. To the best of our knowledge, this is the first normalizing flow model posed in infinite-dimensional spaces.

**Function Space Generative Models.** Recently, a number of authors have proposed function-space generalizations of various deep generative models. Close in spirit to our work are those which generalize diffusion models [Ho et al., 2020, Song et al., 2021, Song and Ermon, 2019] to the infinite-dimensional setting. In particular, Kerrigan et al. [2023] and Lim et al. [2023a] propose function-space generalizations of discrete-time diffusion models, whereas Pidstrigach et al. [2023], Franzese et al. [2023] and Hagemann et al. [2023] propose function-space generalizations of continuous-time diffusion models. Beyond diffusion models, function-space GANs [Rahman et al., 2022] and energy-based models [Lim et al., 2023b] have also been proposed. Our work adds to this growing literature on function-space generative models by proposing the first function-space normalizing flow model.

**Discrete Functional Generative Models.** While there has been growing interest in developing generative models directly in infinite-dimensional spaces, there has also been work proposing generative models for functional data that operate directly on a discretization of the underlying space, for example, diffusion models for time series [Tashiro et al., 2021, Rasul et al., 2021a, Yan et al., 2021] (see Lin et al. [2023] for a recent survey on these methods). Other models, such as normalizing flows [Rasul et al., 2021b], latent variable models [Zhou et al., 2022, Rubanova et al., 2019, Yildiz et al., 2019], and GANs [Yoon et al., 2019, Kidger et al., 2021] have also been explored. However, these methods all operate directly on the discrete observations of a given time series. This has several drawbacks: for instance, it is difficult to transfer a model trained on one discretization to another, and often these models are ill-posed in the functional limit (i.e. as the discretization size goes to zero). In contrast, our work begins from a function-space point of view, where we only discretize in order to perform computations.

# 3 Notation and Background

We begin by introducing some notation and background which we will later use to construct our model. Section 3.1 introduces notions related to flows on function spaces, and Section 3.2 introduces the weak continuity PDE [Stepanov and Trevisan, 2017] which plays a key role in our constructions.

## 3.1 Preliminaries

Let  $\mathcal{X} \subset \mathbb{R}^d$  and consider a real separable Hilbert space  $\mathcal{F}$  of functions  $f: \mathcal{X} \to \mathbb{R}$  equipped with the Borel  $\sigma$ -algebra  $\mathcal{B}(\mathcal{F})$ . We consider the setting where there is a (Borel) probability measure  $\nu$  on  $\mathcal{F}$  from which we have samples, i.e. random functions drawn from the data distribution  $\nu$ . Our goal is to build a generative model which allows us to approximately sample from  $\nu$ . Importantly, any such generative model should be discretization-invariant, in the sense that the model should be able to generate functions which may be observed on any finite but arbitrary discretization of  $\mathcal{X}$ .

In this work, we consider paths of probability measures  $(\mu_t)_{t\in[0,1]}$ , where  $\mu_t\in\mathcal{P}(\mathcal{F})$  is a probability measure on  $\mathcal{F}$  at every time  $t\in[0,1]$ . In particular, we will construct a path of measures which approximately interpolates between a fixed reference measure  $\mu_0$  at time t=0 and the data distribution at time t=1, so that  $\mu_1\approx\nu$ . This interpolation is approximate in the sense that  $\mu_1$  will be a smoothed version of the data distribution, obtained from  $\nu$  via convolution with a Gaussian measure having small variance [Bogachev, 1998, Appendix A].

We consider paths of probability measures which are generated locally, in the sense that there is some underlying time-dependent vector field on  $\mathcal F$  such that the path of measures  $(\mu_t)_{t\in[0,1]}$  is obtained by flowing samples  $g\sim \mu_0$  along said vector field. More formally, a (time-dependent) vector field on  $\mathcal F$  is a mapping  $v:[0,1]\times\mathcal F\to\mathcal F$ . We will often write the time argument as a subscript, so that  $v(t,g)=v_t(g)\in\mathcal F$  can be thought of as a velocity at the point  $g\in\mathcal F$  a time  $t\in[0,1]$ .

The *flow* associated to a vector field  $(v_t)_{t \in [0,1]}$  is the mapping  $\phi : [0,1] \times \mathcal{F} \to \mathcal{F}$  specified by the initial value problem

$$\partial_t \phi_t(q) = v_t(\phi_t(q)) \qquad \phi_0(q) = q \tag{1}$$

where we again write  $\phi(t,g) = \phi_t(g)$  using the time argument as a subscript. As written, Equation (1) represents an ordinary differential equation (ODE) on the abstract and potentially infinite-dimensional space  $\mathcal{F}$ . Such ODEs are often dubbed abstract differential equations [O'Regan, 1997, Zaidman, 1999]. We assume that all vector fields in this work are sufficiently regular such that a solution to Equation (1) is guaranteed to exist for all  $t \in [0,1]$  and  $\nu$ -a.e. initial condition g.

Given any initial probability measure  $\mu_0 \in \mathcal{P}(\mathcal{F})$ , we may consider the path of probability measures generated by the flow  $\phi$ . That is, for any  $t \in [0,1]$  we define the measure  $\mu_t$  via the pushforward of  $\mu_0$  along  $\phi_t$ , i.e.  $\mu_t = [\phi_t]_\# \mu_0$ , where  $\phi_t$  is assumed to be measurable for all  $t \in [0,1]$ .

# 3.2 Weak Continuity PDE

In the previous section, we noted how one may obtain a path of probability measures from an initial probability measure  $\mu_0 \in \mathcal{P}(\mathcal{F})$  by considering the pushforward of  $\mu_0$  along the flow associated to a given vector field  $(v_t)_{t \in [0,1]}$ .

Conversely, we say that the vector field  $(v_t)_{t \in [0,1]}$  generates the path of measures  $(\mu_t)_{t \in [0,1]}$  if the path  $(\mu_t)_{t \in [0,1]}$  is obtained via the pushforward of  $\mu_0$  along the flow associated with  $(v_t)_{t \in [0,1]}$ . Directly verifying whether a vector field generates a given path of measures (by verifying the pushforward relationship) is typically infeasible. Instead, we can check that the two satisfy the *continuity equation* 

$$\partial_t \mu_t + \operatorname{div}(v_t \mu_t) = 0$$
 on  $\mathcal{F} \times [0, 1]$ . (2)

We interpret this PDE in the weak sense [Ambrosio et al., 2005, Ch. 8], by which we mean that the pair  $(v_t)_{t\in[0,1]}$  and  $(\mu_t)_{t\in[0,1]}$  satisfy Equation (2) if

$$\int_{0}^{1} \int_{\mathcal{F}} \left( \partial_{t} \varphi(g, t) + \langle v_{t}(g), \nabla_{g} \varphi(g, t) \rangle \right) d\mu_{t}(g) dt = 0$$
(3)

for all  $\varphi: \mathcal{F} \times [0,1] \to \mathbb{R}$  in some appropriate space of test functions.

We refer to Stepanov and Trevisan [2017, Theorem 3.4] for a rigorous discussion of this result in general metric spaces. Such results are often referred to as *superposition principles*. In the Euclidean setting, if one assumes that all measures admit a density with respect to some common dominating measure, it suffices to check the continuity equation directly, in which  $\mu_t$  is replaced by a density  $p_t$  [Ambrosio et al., 2005, Villani, 2009].

Throughout this work, we assume all paths of measures and vector fields are sufficiently regular such that the superposition principle applies, i.e. it suffices to check the continuity equation to conclude whether a given path of measures is generated by a given vector field. In Theorem 1, we use the weak form of the continuity equation in order to construct a marginal vector field from conditional vector fields, such that this marginal vector field is guaranteed to generate our desired interpolating path of measures.

# 4 Function Space Flow Matching

Building on the notions in Section 3, we now introduce our Functional Flow Matching model (FFM). The Flow Matching model is a recently proposed continuous-time normalizing flow method developed for finite-dimensional spaces [Lipman et al., 2023, Chen and Lipman, 2023]. Our FFM approach builds on this earlier line of work to develop a non-trivial extension of these methods to infinite-dimensional spaces.

The main technical challenge of generalizing the existing techniques to infinite-dimensional spaces is that existing methods rely heavily on the notion of a probability density function, either with respect to the Lebesgue measure in the case of a Euclidean space or with respect to the canonical volume measure on a Riemannian manifold. In infinite-dimensional (Banach) spaces, there does not exist an analogue of the Lebesgue measure – that is, any nonzero translation invariant Borel measure must assign infinite measure to any open set [Eldredge, 2016].

As such, our FFM model necessarily is posed entirely in measure-theoretic terms. Our derivations shed light on strict requirements needed to obtain a well-posed model. For instance, we require an absolute continuity assumption between the conditional and marginal measures defined in Section 4.1. In the Euclidean setting, such assumptions are easy to satisfy, but are non-trivial in infinite-dimensional spaces, even for the simple setting of Gaussian measures (see Section 4.3). Moreover, our derivations demonstrate that naively applying a white-noise Gaussian measure (as is done in the Euclidean setting) leads to an ill-posed model in function space.

# 4.1 Constructing a Path of Measures

Suppose we associate to every  $f \in \mathcal{F}$  a path of measures  $(\mu_t^f)_{t \in [0,1]}$  such that  $\mu_0^f = \mu_0$  is some fixed reference measure and  $\mu_1^f$  is concentrated around f. For instance,  $\mu_1^f$  could be a Gaussian measure with mean f and a covariance having small operator norm. We then marginalize over all such measures, where we mix over the data distribution  $\nu$ . That is, we define a new probability measure  $\mu_t \in \mathcal{P}(\mathcal{F})$  for  $t \in [0,1]$  via

$$\mu_t(A) = \int \mu_t^f(A) \, \mathrm{d}\nu(f) \qquad \forall A \in \mathcal{B}(\mathcal{F}).$$
 (4)

Due to our conditions on  $\mu_t^f$ , we then have that  $\mu_0 = \mu_0$  and  $\mu_1 \approx \nu$  is approximately the data distribution. Suppose further that each conditional path of measures  $\mu_t^f$  is generated by some known vector field  $v_t^f$ . In the following theorem, we claim that we may construct a vector field  $v_t$  which generates the *marginal* path of measures  $\mu_t$  from the conditional vector fields  $v_t^f$ .

#### Theorem 1.

Assume that  $\int_0^1 \int_{\mathcal{F}\times\mathcal{F}} ||v_t^f(g)|| d\mu_t^f(g) d\nu(f) dt < \infty$ . If  $\mu_t^f \ll \mu_t$  for  $\nu$ -a.e. f and almost every  $t \in [0,1]$ , then the vector field

$$v_t(g) = \int_{\mathcal{F}} v_t^f(g) \frac{\mathrm{d}\mu_t^f}{\mathrm{d}\mu_t}(g) \,\mathrm{d}\nu(f) \tag{5}$$

generates the marginal path of measures measure  $(\mu_t)_{t\in[0,1]}$  specified by Equation (4). That is,  $(v_t)_{t\in[0,1]}$  and  $(\mu_t)_{t\in[0,1]}$  solve the continuity equation (2). Here,  $\mathrm{d}\mu_t^f/\mathrm{d}\mu_t$  is the Radon-Nikodym derivative of the conditional measure with respect to the marginal.

*Proof.* Appendix A.1. 
$$\Box$$

If this vector field  $v_t$  were known, we could generate samples by solving the corresponding flow ODE (Equation (1)) with initial condition  $f \sim \mu_0$  drawn from our fixed reference measure. However, the vector field specified by Equation (5) is intractable. Thus, we will learn a model to approximate this unknown vector field. Note that our model will necessarily be a mapping between infinite dimensional spaces. We discuss how to parametrize such a model in Section 5.

The main technical assumption in Theorem 1 is that the conditional distributions  $\mu_t^f$  are  $\nu$ -almost surely absolutely continuous with respect to the marginal distribution  $\mu_t$ . Although this assumption is not generally true even in the Euclidean setting, we prove in Theorem (2) that this assumption holds under an additional equivalency condition on the conditional measures. In Section 4.3, we discuss how this equivalency assumption may be satisfied under a Gaussian parametrization of the model.

## Theorem 2.

Consider a probability measure  $\nu$  on  $\mathcal{F}$  and a collection of measures  $\mu_t^f$  parametrized by  $f \in \mathcal{F}$ . Suppose that the collection of parametrized measures are  $\nu$ -a.e. mutually absolutely continuous. Define the marginal measure  $\mu_t$  via Equation (4). Then, it follows that  $\mu_t^f \ll \mu_t$  for  $\nu$ -a.e. f.

*Proof.* Appendix A.1. 
$$\Box$$

#### 4.2 Special Case: Gaussian Measures

In this section, we specialize to the setting where the reference measure  $\mu_0$  and conditional measures  $\mu_t^f$  are chosen to be Gaussian measures [Bogachev, 1998]. We make this ansatz for several reasons. Foremost, our marginal vector field (Equation (5)) requires an absolute continuity assumption. In infinite-dimensional (separable) Banach spaces, the absolute continuity of Gaussian measures is well-understood, e.g. via the Cameron-Martin theorem and the Feldman-Hájek theorem [Da Prato and Zabczyk, 2014, Bogachev, 1998]. Moreover, we are able to parametrize our Gaussian measures via Gaussian processes [Rasmussen and Williams, 2006, Wild et al., 2022] for which a number of flexible choices of kernels have been explored in the machine learning literature.

More formally, for any  $f \in \mathcal{F}$  we define a conditional path of probability measures  $(\mu_t)_{t \in [0,1]}$  to be a Gaussian measure  $\mu_t^f = \mathcal{N}(m_t^f, C_t^f)$  with mean  $m_t^f \in \mathcal{F}$  and covariance operator  $C_t^f : \mathcal{F} \to \mathcal{F}$ . Note that the  $C_t^f$  are necessarily symmetric, non-negative and trace-class [Da Prato and Zabczyk,

2014, Ch. 2]. In particular, this rules out multiples of the identity operator (corresponding to white noise) as a valid choice for  $C_t^f$ , as these operators are not compact and hence not trace-class.

In practice, we parametrize  $t\mapsto m_t^f$  by a Fréchet differentiable mapping and specify  $C_t^f$  by a covariance operator  $C_0$  and variance schedule  $t\mapsto \sigma_t^f\in\mathbb{R}_{>0}$  such that  $C_t^f=(\sigma_t^f)^2C_0$ . At time t=0, we choose to parametrize  $\mu_0^f=\mu_0=\mathcal{N}(0,C_0)$  as a centered Gaussian measure independent of the function  $f\in\mathcal{F}$ . The measure  $\mu_0$  will serve as the reference measure in our generative model. In order to satisfy the desiderata of Section 4.1, at time t=1 we will choose  $m_1^f=f$  and  $C_t^f$  to have small operator norm so that  $\mu_1^f$  is a Gaussian measure concentrated around f.

In this case, we note that the conditional flow  $\phi^f:[0,1]\times\mathcal{F}\to\mathcal{F}$  defined via

$$\phi_t^f(g) = \sigma_t^f g + m_t^f \tag{6}$$

will push  $g \sim \mathcal{N}(0, C_0)$  to the desired conditional measure  $\mu_t^f$ , i.e.  $\mu_t^f = [\phi_t^f]_\# \mathcal{N}(0, C_0)$ . Using the flow ODE (1), we see that a vector field generating this conditional path of measures is

$$v_t^f(g) = \frac{(\sigma_t^f)'}{\sigma_t^f} (g - m_t^f) + \frac{\mathrm{d}}{\mathrm{d}t} m_t^f \tag{7}$$

where  $(\sigma_t^f)'$  is the ordinary time derivative of the variance schedule and  $d/dt(m_t^f)$  is the Fréchet derivative of the mapping  $t \mapsto m_t^f$ . The proof of this fact is a straightforward generalization of Lipman et al. [2023, Theorem 3], which demonstrates the analogous relationship in finite-dimensional

In this work, we consider the following concrete parametrizations:

**Linear ("OT").** 
$$m_t^f = tf$$
  $\sigma_t^f = 1 - (1 - \sigma_{\min})t$  (8)

Linear ("OT"). 
$$m_t^f = tf$$
  $\sigma_t^f = 1 - (1 - \sigma_{\min})t$  (8)  
Variance Preserving ("VP").  $m_t^f = \alpha_{1-t}f$   $\sigma_t^f = \sqrt{1 - \alpha_{1-t}^2}$  (9)

Here,  $\sigma_{\min} \in \mathbb{R}_{>0}$  and  $\alpha_t \in \mathbb{R}_{>0}$  are hyperparameters of the model controlling the variance of the conditional measures. The "OT" path is named as such as it corresponds to an optimal transport map between Gaussians in the Euclidean setting [Lipman et al., 2023, McCann, 1997], and the variance preserving parametrization is inspired by probability paths defined via diffusion models [Lipman et al., 2023, Song et al., 2021]. We additionally experimented with the "variance exploding" parametrization [Lipman et al., 2023, Song et al., 2021], but found empirically that this was not suitable for our setting. See Appendix A.2 for details.

#### **Absolute Continuity in the Gaussian Setting** 4.3

In general, the absolute continuity assumption of Theorem 1 is difficult to satisfy in function spaces. However, in the Gaussian setting, we may reduce this assumption to assumptions regarding the parametrization of our Gaussian measures. By the Feldman-Hájek theorem [Da Prato and Zabczyk, 2014, Theorem 2.25], our conditional Gaussian measures  $\mu_t^f$  will be mutually absolutely continuous if the difference in means lies in the Cameron-Martin space of  $C_t$ , i.e.  $m_t^f - m_t^g \in C_t^{1/2}(\mathcal{F})$ .

Thus, under suitable assumptions on the data distribution  $\nu$  and an appropriate parametrization of the conditional means, our marginal vector fields (Equation (5)) will be well-defined as a consequence of Theorem 2. Suppose  $C_t = \sigma_t^2 C_0$  is a scaled version of some fixed covariance operator  $C_0$  with the assumption that  $0 < \sigma_t^2 \le M$  is positive and bounded above. By Lemma 6.15 of Stuart [2010], this choice guarantees us that the Cameron-Martin space is constant in time, i.e.  $C_0^{1/2}(\mathcal{F}) = C_t^{1/2}(\mathcal{F})$ for all  $t \in [0, 1]$ .

Assume further that the data distribution is supported on the Cameron-Martin space of  $C_0$ , i.e.  $\nu(C_0^{1/2}(\mathcal{F}))=1.^1$  In this case, given our covariance parametrization, our Gaussian measures will be

Interestingly, this assumption is also made by previous works on function-space diffusion models [Lim et al., 2023a, Kerrigan et al., 2023] – this is perhaps not surprising though, as these works also rely on absolute continuity results for Gaussian measures.

mutually absolutely continuous if e.g.  $m_t^f$  is an affine function of f. We note that the parametrizations suggested in Section 4.2 are all affine, and so under the assumption that the data is supported on the Cameron-Martin space  $C_0^{1/2}(\mathcal{F})$  our setup is well-defined.

In practice, verifying whether the data distribution is supported on  $C_0^{1/2}(\mathcal{F})$  is difficult. One option to guarantee this assumption is satisfied is to pre-process the data via some mapping  $T:\mathcal{F}\to C_0^{1/2}(\mathcal{F})\subseteq \mathcal{F}$  whose image is contained in  $C_0^{1/2}(\mathcal{F})$ . We refer to Appendix C of Lim et al. [2023a] for a further discussion of such mappings and related results. However, we note that in practice, we do not find it necessary to pre-process our data in this manner.

#### 4.4 Training the FFM Model

Ideally, we would like to perform functional regression on the marginal vector field defined via Equation (5), where we approximate  $v_t(q)$  by a model  $u_t(q \mid \theta)$  with parameters  $\theta \in \mathbb{R}^p$ . This could be achieved, for instance, by minimizing the loss

$$\mathcal{L}(\theta) = \mathbb{E}_{t \sim \mathcal{U}[0,1], g \sim \mu_t} \left[ \left\| v_t(g) - u_t(g \mid \theta) \right\|^2 \right]$$
(10)

where  $\mathcal{U}[0,1]$  denotes a uniform distribution over the interval [0,1]. Note here that our model is a mapping  $u: \mathbb{R}^p \times [0,1] \times \mathcal{F} \to \mathcal{F}$ , i.e. our model is a parametrized, time-dependent operator on the function space  $\mathcal{F}$ . However, such a loss is intractable to compute – in fact, we we had access to  $(v_t)_{t\in[0,1]}$ , there would be no need to learn a model. Consider instead the conditional loss, defined via

$$\mathcal{J}(\theta) = \mathbb{E}_{t \sim \mathcal{U}[0,1], f \sim \nu, g \sim \mu_t^f} \left[ \left\| v_t^f(g) - u_t(f \mid \theta) \right\|^2 \right]$$
 (11)

where, rather than regressing on the intractable  $v_t$ , we regress on the known conditional vector fields  $v_t^f$ . In the following theorem, we claim that minimizing  $\mathcal{J}(\theta)$  is equivalent to minimizing  $\mathcal{L}(\theta)$ . This is an infinite-dimensional analogue of Lipman et al. [2023, Theorem 2].

Assume that the true and model vector fields are square-integrable, i.e.  $\int_0^1 \int_{\mathcal{F}} \|v_t(g)\|^2 d\mu_t(g) dt < \infty$  and  $\int_0^1 \int_{\mathcal{F}} \|u_t(g \mid \theta)\|^2 d\mu_t(g) dt < \infty$ . Then, we have that  $\mathcal{L}(\theta) = \mathcal{J}(\theta) + C$  where  $C \in \mathbb{R}$  is a constant independent of  $\theta$ .

*Proof.* Appendix A.1. 
$$\Box$$

# **Experiments**

The following section is devoted to demonstrating the empirical performance of FFM on unconditional and conditional tasks. In all settings, we assume we are working in the space  $\mathcal{F} = L^2([0,1])$ . The neural architecture we use to implement  $(u_t(-\mid \theta))_{t\in[0,1]}$  is the Fourier Neural Operator (FNO), introduced by Li et al. [2021]. Once the model is trained, sampling can be achieved by deploying an ODE solver that uses the learned vector field to map samples from a Gaussian measure to our target distribution. In our implementation, we use the DOPRI method [Dormand and Prince, 1980] to perform this task. Additional details can be found in Appendix A.2. Code for all of our experiments will be made available upon publication.

**AEMET dataset.** This dataset consists of a set of functions describing the mean curve of the average daily temperature (in Celsius) for the period 1980-2009 recorded by 73 weather stations in Spain [Febrero-Bande and de la Fuente, 2012]. Each function is observed on a uniform grid at a resolution of 365. We use an FNO with a width of 256 and 64 modes across all experiments. We include experiments on an additional synthetic dataset in Appendix A.3.

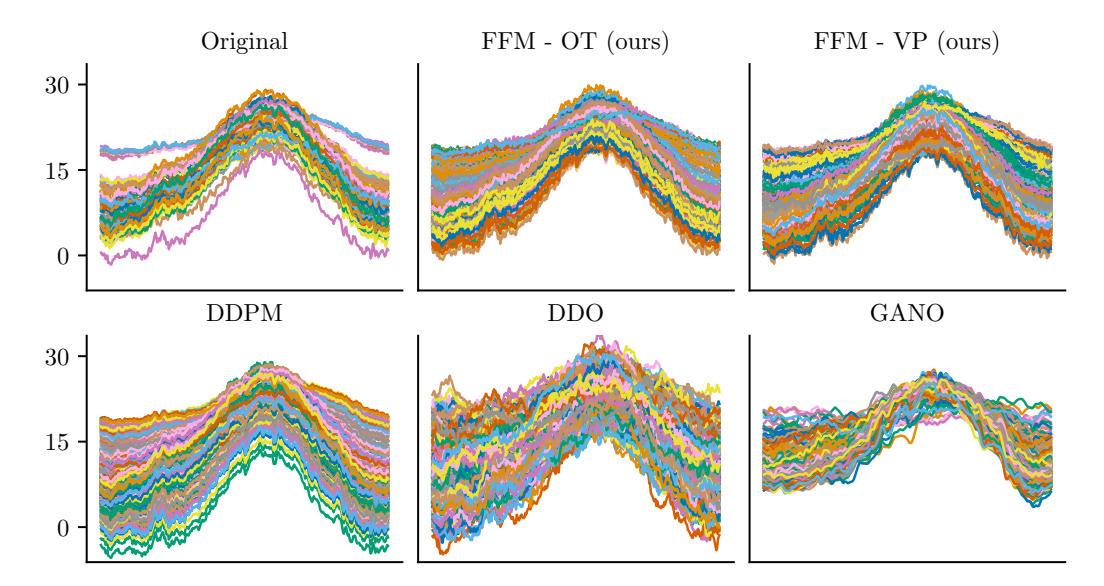


Figure 2: Unconditional generation of 500 samples from various models trained on the AEMET dataset. Samples from our FFM model and DDPM appear visually to better match the characteristics of the real data (top left) relative to DDO and GANO. However, in terms of quantitative results (Table 1) our FFM methods are significantly better than any baselines.

Table 1: Average MSEs between true and generated samples for various pointwise statistics on AEMET, along with minimum and maximum values reported across ten random seeds. Variants of our proposed FFM model obtain the best average performance across all metrics.

	Mean	Variance	Skew	Kurtosis	Autocorr.
FFM-OT (ours)	8.4e-2 (1.3e-2,3.2e-1)	1.7e+0 (1.2e-1,4.0e+0)	3.3e-2 (3.4e-3,1.1e-1)	7.7e-2 (1.3e-2,2.2e-1)	<b>3.0e-6</b> (0.0e+0,1.1e-5)
FFM-VP (ours)	1.3e-1 (3.9e-3,5.0e-1)	1.5e+0 (9.1e-2,3.3e+0)	1.7e-2 (5.4e-3,4.6e-2)	5.0e-2 (1.0e-2,1.5e-1)	6.0e-6 (0.0e+0,1.6e-5)
DDPM	3.0e-1 (3.6e-3,8.2e-1)	3.5e+0 (5.7e-1,1.6e+1)	4.8e-2 (4.7e-3,1.0e-1)	2.2e-1 (3.3e-2,8.0e-1)	1.2e-5 (2.0e-6,3.0e-5)
DDO	2.4e-1 (2.3e-2,4.7e-1)	6.6e+0 (1.0e+0,1.4e+1)	3.8e-2 (2.5e-2,6.1e-2)	2.1e-1 (1.5e-1,3.0e-1)	6.7e-4 (4.8e-4,8.1.0e-4)
GANO	6.5e+1 (9.2e-1,6.2e+2)	3.7e+1 (2.8e+0,1.4e+2)	3.3e-1 (5.9e-2,1.2e+0)	2.9e+0 (1.8e-1,1.5e+1)	1.2e-3 (3.4e-5,1.0e-2)

# 5.1 Unconditional Generation

To accomplish unconditional generation tasks, the FFM model is trained using the OT and VP parametrizations. The functions defining the conditional paths are detailed in (8) and (9) respectively, and in both cases we minimize the conditional loss  $\mathcal{J}(\theta)$  defined in (11). We compare against several functional generative models as baselines, including the Denoising Diffusion Operator (DDO) [Lim et al., 2023a] with NCSN noise scale, GANO [Rahman et al., 2022], and functional DDPM [Kerrigan et al., 2023]. We opt to not compare with non-functional methods, as we are primarily interested in developing discretization-invariant generative models. For each model, we specify all noise via a Gaussian process with a Matérn kernel (see Appendix A.2). Each model is trained for 50 epochs and error bands are computed by reporting intervals across ten random seeds.

In Figure 2, we plot both the original data and samples from the various models considered. We see that our methods (FFM-OT and FFM-VP) are able to produce samples which qualitatively match the original data. In addition, in Table 1, we quantitatively compare our model against the considered baselines by computing various pointwise statistics of the generated functions and computing the MSE between these pointwise statistics and those of the real data. Our FFM models perform the best, on average, in all metrics considered.

# 5.2 Conditional Generation

In addition to unconditional generation of functions, we demonstrate that our method can be extended to perform conditional generation. That is, we have access to side information  $z \in \mathbb{R}^d$  (assumed to be finite dimensional) and we are interested in sampling from the conditional data measure  $\nu(df \mid z)$ .

For instance, z could be a collection of observed values of some function, and we may be interesting in generating functions which interpolate (or extrapolate) these given observations. We describe two approaches to performing conditional generation: one based on a modified training process, and a second based on a modified sampling process. In Figure 3, we demonstrate these two approaches.

Conditional Training. Using the unconditional paths of measures  $\mu_t^f$  as described in the unconditional setting, we may define a conditional marginal  $\mu_t(\operatorname{d} f \mid z)$  by mixing over  $\operatorname{d}\nu(f \mid z)$ , i.e.  $\mu_t(A \mid z) := \int_{\mathcal{F}} \mu_t^f(A) \operatorname{d}\nu(f \mid z)$ .

As long as  $\mu_t^f$  is concentrated around f, then  $\mu_t(\mathrm{d}f \mid z) \approx \nu(\mathrm{d}f \mid z)$ . Note that this condition is satisfied for the paths of measures constructed for unconditional generation, and hence no modification is necessary. However, modifying the conditional measures to account for the information z could potentially be beneficial, and we leave exploration of such design choices to future work. In all, we obtain a modified loss function

$$\mathcal{J}_{\mathcal{C}}(\theta) = \mathbb{E}_{t \sim \mathcal{U}[0,1], z \sim q(z), f \sim \nu(\operatorname{d}f|z), g \sim \mu_t^f} \left[ \left\| v_t^f(g) - u_t(f \mid z, \theta) \right\|^2 \right]. \tag{12}$$

In other words, we simply adapt our model architecture to also take in conditioning information z at training time. In practice, because z is assumed to be finite dimensional, we concatenate z to the input of our FNO model [Li et al., 2021]. We note that a similar loss appears in the context of Flow Matching generative models for video, as proposed by [Davtyan et al., 2022].

**Conditional Sampling.** As an alternative, we may instead modify the sampling process to account for z. This allows one to train an unconditional model and sample conditionally at generation time (in contrast to the conditional training setup, which only allows you to condition on the particular form of z you have trained on). Here, we assume that  $z=(\vec{x},\vec{y})$  consists of a collection of function observations, and that we would like to generate functions whose values match those observed in z.

In order to achieve this, at time  $t \in [0,1]$ , we take a step as dictated by our ODE solver and model vector field to obtain a function  $\tilde{f}_t$ . Next, we flow the information contained in z forwards for t seconds along the conditional vector field designated by our model to obtain  $z_t = (\vec{x}, \vec{y}_t)$ . Then, we set  $f_t(\vec{x}) = \vec{y}_t$ . This approach can be seen as an extension of the ILVR method, which has been successfully applied to diffusion models for conditional image generation [Choi et al., 2021] and diffusion models for conditional function generation [Kerrigan et al., 2023].

# 6 Conclusion

We introduce Functional Flow Matching (FFM), a continuous-time normalizing flow model

which allows us to model distributions supported on infinite-dimensional Hilbert spaces. Importantly, our method is simulation-free, allowing for efficient training and scaling to high-resolution datasets. Empirically, we demonstrate that FFM is able to outperform several recently proposed function-space generative models in terms of sample quality. Our work builds the foundations for function-space normalizing flows, and in future work, these constructions may be extended to other practical instantiations of such models.

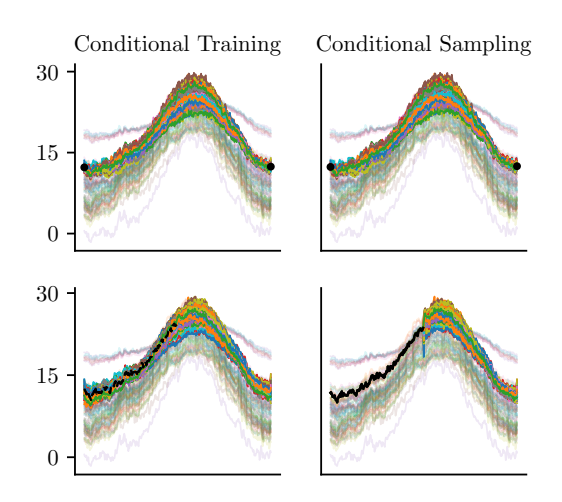


Figure 3: Conditional samples from the FFM-OT model. Darker curves indicate samples and lighter curves depict real data. Conditioning information is shown in black. The first column corresponds to a conditionally trained model and the second column corresponds to a conditionally trained model in addition to conditional sampling. We see that, while the conditionally trained model takes into account the conditioning information, the conditional sampling method allows us to enforce equality of the generated samples to the conditioning information at the observation locations.

**Broader Impacts & Limitations.** As with any other generative model, proliferation of generated samples as if they were real may lead to negative societal outcomes. Although the negative impact of this for time-series is less clear than that of, say, image data, our methodology potentially can be extended to the generation of images at arbitrary resolution.

In terms of limitations, our model is implemented via the FNO [Li et al., 2021], which can only handle data which is discretized on a uniform grid. Exploring different model architectures which relax this assumption is an interesting direction for future work. An additional limitation of our work is that there is no established benchmark for functional generation, unlike say FID [Heusel et al., 2017] for images. Developing benchmarks and metrics for these tasks is an important direction for later work in this area.

**Acknowledgements.** This research was supported in part by the Hasso Plattner Institute (HPI) Research Center in Machine Learning and Data Science at the University of California, Irvine, by NSF under awards 1900644 and 1927245, and by the National Institute of Health under awards R01-AG065330-02S1 and R01-LM013344.

#### References

- Michael Samuel Albergo and Eric Vanden-Eijnden. Building normalizing flows with stochastic interpolants. In *International Conference on Learning Representations*, 2023.
- Luigi Ambrosio, Nicola Gigli, and Giuseppe Savaré. *Gradient Flows: In Metric Spaces and in the Space of Probability Measures.* Springer Science & Business Media, 2005.
- Heli Ben-Hamu, Samuel Cohen, Joey Bose, Brandon Amos, Maximillian Nickel, Aditya Grover, Ricky T. Q. Chen, and Yaron Lipman. Matching normalizing flows and probability paths on manifolds. In *International Conference on Machine Learning*, volume 162, pages 1749–1763, 2022.
- Vladimir Igorevich Bogachev. Gaussian Measures. American Mathematical Society, 1998.
- Ricky T. Q. Chen. torchdiffeq, 2018. URL https://github.com/rtqichen/torchdiffeq.
- Ricky T. Q. Chen, Yulia Rubanova, Jesse Bettencourt, and David K Duvenaud. Neural ordinary differential equations. In *Advances in Neural Information Processing Systems*, volume 31, 2018.
- Ricky TQ Chen and Yaron Lipman. Riemannian flow matching on general geometries. *arXiv preprint* arXiv:2302.03660, 2023.
- Jooyoung Choi, Sungwon Kim, Yonghyun Jeong, Youngjune Gwon, and Sungroh Yoon. ILVR: conditioning method for denoising diffusion probabilistic models. In *Proceedings of the IEEE/CVF International Conference on Computer Vision*, pages 14367–14376, 2021.
- Giuseppe Da Prato and Jerzy Zabczyk. Stochastic Equations in Infinite Dimensions. Cambridge University Press, 2014.
- Aram Davtyan, Sepehr Sameni, and Paolo Favaro. Randomized conditional flow matching for video prediction. *arXiv preprint arXiv:2211.14575*, 2022.
- Prafulla Dhariwal and Alexander Nichol. Diffusion models beat GANs on image synthesis. In *Advances in Neural Information Processing Systems*, volume 34, pages 8780–8794, 2021.
- J.R. Dormand and P.J. Prince. A family of embedded Runge-Kutta formulae. *Journal of Computational and Applied Mathematics*, 6:19–26, 1980.
- Nathaniel Eldredge. Analysis and probability on infinite-dimensional spaces. *arXiv preprint arXiv:1607.03591*, 2016.
- Manuel Febrero-Bande and Manuel Oviedo de la Fuente. Statistical computing in functional data analysis: The R package fda.usc. *Journal of Statistical Software*, 51:1–28, 2012.

- Giulio Franzese, Simone Rossi, Dario Rossi, Markus Heinonen, Maurizio Filippone, and Pietro Michiardi. Continuous-time functional diffusion processes. *arXiv preprint arXiv:2303.00800*, 2023.
- Karan Goel, Albert Gu, Chris Donahue, and Christopher Ré. It's raw! Audio generation with state-space models. In *International Conference on Machine Learning*, pages 7616–7633, 2022.
- Paul Hagemann, Lars Ruthotto, Gabriele Steidl, and Nicole Tianjiao Yang. Multilevel diffusion: Infinite dimensional score-based diffusion models for image generation. *arXiv* preprint arXiv:2303.04772, 2023.
- Martin Heusel, Hubert Ramsauer, Thomas Unterthiner, Bernhard Nessler, and Sepp Hochreiter. GANs trained by a two time-scale update rule converge to a local Nash equilibrium. In *Advances in Neural Information Processing Systems*, volume 30, 2017.
- Jonathan Ho, Ajay Jain, and Pieter Abbeel. Denoising diffusion probabilistic models. In *Advances in Neural Information Processing Systems*, volume 33, pages 6840–6851, 2020.
- Jonathan Ho, William Chan, Chitwan Saharia, Jay Whang, Ruiqi Gao, Alexey Gritsenko, Diederik P Kingma, Ben Poole, Mohammad Norouzi, David J. Fleet, and Tim Salimans. Imagen video: High definition video generation with diffusion models. *arXiv preprint arXiv:2210.02303*, 2022.
- Minguk Kang, Jun-Yan Zhu, Richard Zhang, Jaesik Park, Eli Shechtman, Sylvain Paris, and Taesung Park. Scaling up GANs for text-to-image synthesis. *arXiv preprint arXiv:2303.05511*, 2023.
- Gavin Kerrigan, Justin Ley, and Padhraic Smyth. Diffusion generative models in infinite dimensions. In *International Conference on Artificial Intelligence and Statistics*, volume 206, pages 9538–9563, 2023.
- Patrick Kidger, James Foster, Xuechen Li, and Terry J Lyons. Neural SDEs as infinite-dimensional GANs. In *International Conference on Machine Learning*, volume 139, pages 5453–5463, 2021.
- Ivan Kobyzev, Simon J.D. Prince, and Marcus A. Brubaker. Normalizing flows: An introduction and review of current methods. *IEEE transactions on Pattern Analysis and Machine Intelligence*, 43: 3964–3979, 2020.
- Zhifeng Kong, Wei Ping, Jiaji Huang, Kexin Zhao, and Bryan Catanzaro. Diffwave: A versatile diffusion model for audio synthesis. In *International Conference on Learning Representations*, 2021.
- Zongyi Li, Nikola Borislavov Kovachki, Kamyar Azizzadenesheli, Burigede liu, Kaushik Bhattacharya, Andrew Stuart, and Anima Anandkumar. Fourier neural operator for parametric partial differential equations. In *International Conference on Learning Representations*, 2021.
- Jae Hyun Lim, Nikola B Kovachki, Ricardo Baptista, Christopher Beckham, Kamyar Azizzadenesheli, Jean Kossaifi, Vikram Voleti, Jiaming Song, Karsten Kreis, Jan Kautz, Chrisotopher Pal, Arash Vahdat, and Anima Anandkumar. Score-based diffusion models in function space. arXiv preprint arXiv:2302.07400, 2023a.
- Jen Ning Lim, Sebastian Vollmer, Lorenz Wolf, and Andrew Duncan. Energy-based models for functional data using path measure tilting. In *International Conference on Artificial Intelligence and Statistics*, pages 1904–1923, 2023b.
- Lequan Lin, Zhengkun Li, Ruikun Li, Xuliang Li, and Junbin Gao. Diffusion models for time series applications: A survey. *arXiv preprint arXiv:2305.00624*, 2023.
- Yaron Lipman, Ricky T. Q. Chen, Heli Ben-Hamu, Maximilian Nickel, and Matthew Le. Flow matching for generative modeling. In *International Conference on Learning Representations*, 2023.
- Xingchao Liu, Chengyue Gong, and Qiang Liu. Flow straight and fast: Learning to generate and transfer data with rectified flow. *arXiv preprint arXiv:2209.03003*, 2022.
- Robert J McCann. A convexity principle for interacting gases. *Advances in Mathematics*, 128(1): 153–179, 1997.

- Kirill Neklyudov, Daniel Severo, and Alireza Makhzani. Action matching: A variational method for learning stochastic dynamics from samples. *arXiv preprint arXiv:2210.06662*, 2022.
- Alexander Quinn Nichol and Prafulla Dhariwal. Improved denoising diffusion probabilistic models. In *International Conference on Machine Learning*, pages 8162–8171, 2021.
- Donal O'Regan. Differential Equations in Abstract Spaces, pages 186–194. Springer Netherlands, 1997.
- George Papamakarios, Eric Nalisnick, Danilo Jimenez Rezende, Shakir Mohamed, and Balaji Lakshminarayanan. Normalizing flows for probabilistic modeling and inference. *The Journal of Machine Learning Research*, 22:2617–2680, 2021.
- Jakiw Pidstrigach, Youssef Marzouk, Sebastian Reich, and Sven Wang. Infinite-dimensional diffusion models for function spaces. *arXiv preprint arXiv:2302.10130*, 2023.
- Md Ashiqur Rahman, Manuel A Florez, Anima Anandkumar, Zachary E Ross, and Kamyar Azizzadenesheli. Generative adversarial neural operators. *Transactions on Machine Learning Research*, 2022. ISSN 2835-8856.
- Carl Edward Rasmussen and Christopher Williams. *Gaussian Processes for Machine Learning*. Springer, 2006.
- Kashif Rasul, Calvin Seward, Ingmar Schuster, and Roland Vollgraf. Autoregressive denoising diffusion models for multivariate probabilistic time series forecasting. In *International Conference on Machine Learning*, pages 8857–8868, 2021a.
- Kashif Rasul, Abdul-Saboor Sheikh, Ingmar Schuster, Urs M Bergmann, and Roland Vollgraf. Multivariate probabilistic time series forecasting via conditioned normalizing flows. In *International Conference on Learning Representations*, 2021b.
- Yulia Rubanova, Ricky T. Q. Chen, and David K. Duvenaud. Latent ordinary differential equations for irregularly-sampled time series. In Advances in Neural Information Processing Systems, volume 32, 2019.
- Chitwan Saharia, William Chan, Saurabh Saxena, Lala Li, Jay Whang, Emily L Denton, Kamyar Ghasemipour, Raphael Gontijo Lopes, Burcu Karagol Ayan, Tim Salimans, Jonathan Ho, David J. Fleet, and Mohammad Norouzi. Photorealistic text-to-image diffusion models with deep language understanding. In *Advances in Neural Information Processing Systems*, volume 35, pages 36479–36494, 2022.
- Yang Song and Stefano Ermon. Generative modeling by estimating gradients of the data distribution. In *Advances in Neural Information Processing Systems*, volume 32, 2019.
- Yang Song, Jascha Sohl-Dickstein, Diederik P Kingma, Abhishek Kumar, Stefano Ermon, and Ben Poole. Score-based generative modeling through stochastic differential equations. In *International Conference on Learning Representations*, 2021.
- Eugene Stepanov and Dario Trevisan. Three superposition principles: currents, continuity equations and curves of measures. *Journal of Functional Analysis*, 272(3):1044–1103, 2017.
- Andrew M. Stuart. Inverse problems: a Bayesian perspective. Acta Numerica, 19:451–559, 2010.
- Yusuke Tashiro, Jiaming Song, Yang Song, and Stefano Ermon. CSDI: Conditional score-based diffusion models for probabilistic time series imputation. In *Advances in Neural Information Processing Systems*, volume 34, pages 24804–24816, 2021.
- Cédric Villani. Optimal Transport: Old and New. Springer Berlin Heidelberg, 2009.
- Veit David Wild, Robert Hu, and Dino Sejdinovic. Generalized variational inference in function spaces: Gaussian measures meet Bayesian deep learning. In *Advances in Neural Information Processing Systems*, volume 35, pages 3716–3730, 2022.

- Tijin Yan, Hongwei Zhang, Tong Zhou, Yufeng Zhan, and Yuanqing Xia. Scoregrad: Multivariate probabilistic time series forecasting with continuous energy-based generative models. *arXiv* preprint arXiv:2106.10121, 2021.
- Cagatay Yildiz, Markus Heinonen, and Harri Lahdesmaki. ODE2VAE: Deep generative second order ODEs with Bayesian neural networks. In *Advances in Neural Information Processing Systems*, volume 32, 2019.
- Jinsung Yoon, Daniel Jarrett, and Mihaela van der Schaar. Time-series generative adversarial networks. In *Advances in Neural Information Processing Systems*, volume 32, 2019.
- Samuel Zaidman. Functional Analysis and Differential Equations in Abstract Spaces. Taylor & Francis, 1999.
- Linqi Zhou, Michael Poli, Winnie Xu, Stefano Massaroli, and Stefano Ermon. Deep latent state space models for time-series generation. *arXiv preprint arXiv:2212.12749*, 2022.

# A.1 Proofs of Theorems

#### Theorem 1.

Assume that  $\int_0^1 \int_{\mathcal{F}\times\mathcal{F}} ||v_t^f(g)|| d\mu_t^f(g) d\nu(f) dt < \infty$ . If  $\mu_t^f \ll \mu_t$  for  $\nu$ -a.e. f and almost every  $t \in [0,1]$ , then the vector field

$$v_t(g) = \int_{\mathcal{F}} v_t^f(g) \frac{\mathrm{d}\mu_t^f}{\mathrm{d}\mu_t}(g) \,\mathrm{d}\nu(f) \tag{5}$$

generates the marginal path of measures measure  $(\mu_t)_{t\in[0,1]}$  specified by Equation (4). That is,  $(v_t)_{t\in[0,1]}$  and  $(\mu_t)_{t\in[0,1]}$  solve the continuity equation (2). Here,  $\mathrm{d}\mu_t^f/\mathrm{d}\mu_t$  is the Radon-Nikodym derivative of the conditional measure with respect to the marginal.

*Proof.* We show that for an arbitrary but fixed test function  $\varphi$ ,

$$\int_{0}^{1} \int_{\mathcal{F}} \partial_{t} \varphi(g, t) \, \mathrm{d}\mu_{t}(g) \, \mathrm{d}t = -\int_{0}^{1} \int_{\mathcal{F}} \langle v_{t}(g), \nabla_{g} \varphi(g, t) \, \mathrm{d}\mu_{t}(g) \, \mathrm{d}t. \tag{13}$$

To that end, we begin by analyzing the left-hand side, replacing the integration of the marginal measure  $\mu_t$  with a double integral over its components:

$$\int_{0}^{1} \int_{\mathcal{F}} \partial_{t} \varphi(g, t) \, \mathrm{d}\mu_{t}(g) \, \mathrm{d}t = \int_{0}^{1} \int_{\mathcal{F}} \int_{\mathcal{F}} \partial_{t} \varphi(g, t) \, \mathrm{d}\mu_{t}^{f}(g) \, \mathrm{d}\nu(f) \, \mathrm{d}t \tag{14}$$

By Fubini-Tonelli and using the assumption that  $v_t^f$  generates  $\mu_t^f$ , we obtain via the continuity equation for  $(v_t^f, \mu_t^f)$ :

$$= -\int_{\mathcal{T}} \int_{0}^{1} \int_{\mathcal{T}} \langle v_{t}^{f}(g), \nabla_{g} \varphi(g, t) \rangle \, \mathrm{d}\mu_{t}^{f}(g) \, \mathrm{d}t \, \mathrm{d}\nu(f) \tag{15}$$

Using our absolute continuity assumption and Fubini-Tonelli once again, we perform a change of measure to obtain

$$= -\int_{0}^{1} \int_{\mathcal{F}} \int_{\mathcal{F}} \langle v_{t}^{f}(g), \nabla_{g} \varphi(g, t) \rangle \frac{\mathrm{d}\mu_{t}^{f}}{\mathrm{d}\mu_{t}}(g) \, \mathrm{d}\mu_{t}(g) \, \mathrm{d}\nu(f) \, \mathrm{d}t$$
 (16)

$$= -\int_{0}^{1} \int_{\mathcal{F}} \int_{\mathcal{F}} \langle v_{t}^{f}(g) \frac{\mathrm{d}\mu_{t}^{f}}{\mathrm{d}\mu_{t}}(g), \nabla_{g}\varphi(g, t) \rangle \,\mathrm{d}\mu_{t}(g) \,\mathrm{d}\nu(f) \,\mathrm{d}t$$
 (17)

Using the fact that Bochner integrals commute with inner products,

$$= -\int_0^1 \int_{\mathcal{F}} \left\langle \int_{\mathcal{F}} v_t^f(g) \frac{\mathrm{d}\mu_t^f}{\mathrm{d}\mu_t}(g) \,\mathrm{d}\nu(f), \nabla_f \varphi(f, t) \right\rangle \,\mathrm{d}\mu_t(g) \,\mathrm{d}t \tag{18}$$

$$= -\int_0^1 \int_{\mathcal{F}} \langle v_t(g), \nabla_f \varphi(f, t) \rangle \, d\mu_t(g) \, dt \tag{19}$$

Hence, we have shown that the vector field generating  $\mu_t$  is given by

$$v_t(g) = \int_{\mathcal{T}} v_t^f(g) \frac{\mathrm{d}\mu_t^f}{\mathrm{d}\mu_t}(g) \,\mathrm{d}\nu(f). \tag{20}$$

### Theorem 2.

Consider a probability measure  $\nu$  on  $\mathcal{F}$  and a collection of measures  $\mu_t^f$  parametrized by  $f \in \mathcal{F}$ . Suppose that the collection of parametrized measures are  $\nu$ -a.e. mutually absolutely continuous. Define the marginal measure  $\mu_t$  via Equation (4). Then, it follows that  $\mu_t^f \ll \mu_t$  for  $\nu$ -a.e. f.

*Proof.* By assumption, there exists  $\mathcal{G} \subset \mathcal{F}$  with  $\nu(G) = 1$  and for any  $f,g \in \mathcal{G}$ , we have  $\mu^f \ll \mu^g$  and  $\mu^g \ll \mu^f$ . Fix  $A \in \mathcal{B}(\mathcal{F})$  with  $\mu(A) = 0$ . We claim that  $\mu^f(A) = 0$  for every  $f \in \mathcal{G}$ . Note that as  $\mathcal{G} \subset \mathcal{F}$  has full measure, the integral defining  $\mu$  may be taken over  $\mathcal{G}$  rather than  $\mathcal{F}$ . Suppose for the sake of contradiction that  $\mu^f(A) > 0$  for some  $f \in \mathcal{G}$ . From the mutual equivalencies of the measures parametrized by  $\mathcal{G}$ , it follows that  $\mu^g(A) > 0$  for every  $g \in \mathcal{G}$ . Given the form of the mixture measure  $\mu$ , it would then follow that  $\mu(A) > 0$ , which is a contradiction. Thus,  $\mu^f \ll \mu$  for  $\nu$ -a.e. f as claimed.

#### Theorem 3.

Assume that the true and model vector fields are square-integrable, i.e.  $\int_0^1 \int_{\mathcal{F}} \|v_t(g)\|^2 d\mu_t(g) dt < \infty$  and  $\int_0^1 \int_{\mathcal{F}} \|u_t(g \mid \theta)\|^2 d\mu_t(g) dt < \infty$ . Then, we have that  $\mathcal{L}(\theta) = \mathcal{J}(\theta) + C$  where  $C \in \mathbb{R}$  is a constant independent of  $\theta$ .

*Proof.* First, note that since we are working in a real Hilbert space, for fixed  $f, g \in \mathcal{F}$  we have

$$\|v_t(g) - u_t(g \mid \theta)\|^2 = \langle v_t(g) - u_t(g \mid \theta), v_t(g) - u_t(g \mid \theta) \rangle$$
(21)

$$= \|v_t(g)\|^2 + \|u_t(g \mid \theta)\|^2 - 2\langle v_t(g), u_t(g \mid \theta)\rangle$$
 (22)

and similarly,

$$\|v_t^f(g) - u_t(g \mid \theta)\|^2 = \|v_t^f(g)\|^2 + \|u_t(g \mid \theta)\|^2 - 2\langle v_t(g), u_t(g \mid \theta)\rangle.$$
 (23)

The first term in both is independent of the model parameters  $\theta$ . We analyze the remaining two terms. First, using the fact that  $\mu_t$  is a mixture measure,

$$\mathbb{E}_{t,\mu_t} \left[ \| u_t(g \mid \theta) \|^2 \right] = \int_0^1 \int_{\mathcal{F}} \| u_t(g \mid \theta) \|^2 \, \mathrm{d}\mu_t(g) \, \mathrm{d}t$$
 (24)

$$= \int_0^1 \int_{\mathcal{F}} \int_{\mathcal{F}} \|u_t(g \mid \theta)\|^2 d\mu_t^f(g) d\nu(f) dt$$
 (25)

$$= \mathbb{E}_{t,g \sim \mu_t^f, f \sim \nu} \left[ \left\| u_t(g \mid \theta) \right\|^2 \right]. \tag{26}$$

Next, using the exchangeability between Bochner integrals and inner products, and several applications of Fubini-Tonelli,

$$\mathbb{E}_{t,g \sim \mu_t} \left[ \langle v_t(g), u_t(g \mid \theta) \right] = \int_0^1 \int_{\mathcal{F}} \langle v_t(g), u_t(g \mid \theta) \rangle \, \mathrm{d}\mu_t \, \mathrm{d}t$$
 (27)

$$= \int_0^1 \int_{\mathcal{F}} \left\langle \int_{\mathcal{F}} v_t^f(g) \frac{\mathrm{d}\mu_t^f}{\mathrm{d}\mu_t}(g) \,\mathrm{d}\nu(f), u_t(g \mid \theta) \right\rangle \,\mathrm{d}\mu_t(g) \,\mathrm{d}t \tag{28}$$

$$= \int_0^1 \int_{\mathcal{F}} \int_{\mathcal{F}} \langle v_t^f(g), u_t(g \mid \theta) \rangle \frac{d\mu_t^f}{d\mu_t}(g) \, d\mu_t(g) \, d\nu(f) \, dt$$
 (29)

$$= \int_0^1 \int_{\mathcal{F}} \int_{\mathcal{F}} \langle v_t^f(g), u_t(g \mid \theta) \, \mathrm{d}\mu_t^f(g) \, \mathrm{d}\nu(f) \, \mathrm{d}t$$
 (30)

$$= \mathbb{E}_{t, f \sim \nu, g \sim \mu_t^f} \left[ \langle v_t^f(g), u_t(g \mid \theta) \rangle \right]. \tag{31}$$

This shows the equivalency of the two losses.

# A.2 Experiment Details

### A.2.1 Parametrizations

The FM-OT and FM-VP model require specifying a variance schedule via the hyperparameter  $\sigma_t^f$ . In this work, we parametrize FFM-OT by setting  $\sigma_{\min} = 1\mathrm{e}-4$ . For FFM-VP, we set  $\alpha_t = \cos\left(\frac{t+s}{1+s}\frac{\pi}{2}\right)$  where s=0.08, following a formulation similar to the cosine schedule introduced by Nichol and Dhariwal [2021].

For the baseline models considered (DDPM [Kerrigan et al., 2023], DDO [Lim et al., 2023a], GANO [Rahman et al., 2022]), we use the hyperparameters suggested by the original papers, other than the model architecture which is fixed across all experiments.

# A.2.2 Training Details

Each model experimented with relies on noise sampled from a Gaussian measure. In our work, we consider a mean-zero Gaussian process (GP) parametrized by a Matérn kernel with  $\nu=1/2$ , length scale  $\ell=0.1$ , and variance  $\sigma^2=0.1$ .

As mentioned in Section 5, we use a Fourier Neural Operator [Li et al., 2021] with a fixed architecture for every model in each of our experiments. Specifically, we include an initial layer lifting the dimensionality of the discretized function to a desired width (fixed at 256 for the AEMET dataset, and at 128 for the MoGP synthetic dataset described below), four Fourier layers (64 modes for the AEMET dataset, 32 for the MoGP dataset) with GELU activation function, and two final hidden layers. For GANO, both the discriminator and the generator follow the same parametrization. All models are trained for 50 epochs, using the Adam optimizer with an initial learning rate of 1e-3, scheduled to be rescaled to

	Training	Sampling
FFM-OT (ours)	1.9479e-1	1.6041e-1
FFM-VP (ours)	1.9487e-1	1.5623e-1
DDPM	1.9620e-1	3.2684e-1
NCSN	1.9609e-1	6.5091e-1
GANO	1.4798e+0	3.5316e-4

Table 2: Training and sampling time of 1000 samples in GPU hours on an NVIDIA GeForce RTX 2080 Ti, for the models considered in the AEMET experiment.

1e-4 after 25 epochs. Moreover, we set a weight decay  $L^2$  penalty of 1e-4. The batch size is set to 73 for the AEMET dataset, and to 64 for the MoGP dataset. As a reference, the training times of all the models used in the AEMET dataset are reported in Table 2.

# A.2.3 Sampling Details

We use the torchdiffeq [Chen, 2018] package for all ODE solvers. The specific solver we use is dopri5, an implementation of the Dormand-Prince method [Dormand and Prince, 1980] of order 5. We set the absolute and relative tolerance parameters to 1e-10. Sampling times for 1000 samples from all of the models used in the experiment on the AEMET dataset are reported in Table 2.

# A.3 Additional Experimental Results

## A.3.1 Additional Results: MoGP

Mixture of Gaussian Processes (MoGP) Dataset. The experiment considers the task of generating samples from a mixture of two GPs. The two components, with equal weights, have mean functions  $m_1=10x-5$  and  $m_2=-10x+5$ , and a squared-exponential kernel with variance  $\sigma^2=0.04$  and length scale  $\ell=0.1$ . The synthetic samples used for training are observed on a uniform grid at a resolution of 64 on the interval [0,1]. All models were trained on the same sample of N=5000 realizations of the mixture of GPs. Figure 4 illustrates a visual comparison of 500 samples from each model, while Table 3 presents a quantitative comparison of the mean squared error (MSE) on various pointwise statistics. Additionally, Figure 5 provides a comprehensive depiction of the variations in these pointwise statistics across different models. The same plot is provided for the experiments on the AEMET dataset in Figure 6.

Table 3: Average MSEs between true and generated samples for various pointwise statistics on the MoGP dataset, along with minimum and maximum values reported across ten random seeds. Variants of our proposed FFM model obtain the best or second best average performance across all metrics. The DDPM model outperforms the FFM variants in terms of variance, but only by a small margin.

	1				
	Mean	Variance	Skew	Kurtosis	Autocorr.
FFM-OT (ours)	2.2e-2 (2.6e-3,9.5e-2)	3.6e-1 (6.e-2,9.1e-1)	1.2e-2 (1.8e-3,4.4e-2)	1.0e-2 (1.5e-3,1.4e-2)	<b>5.e-6</b> (2.e-6,1.e-5)
FFM-VP (ours)	3.9e-2 (2.8e-3,1.1e-1)	4.4e-1 (1.7e-2,2.2e+0)	1.6e-2 (3.5e-3,3.8e-2)	<b>5.8e-3</b> (2.0e-3,1.3e-2)	6.e-6 (2.e-6,1.2e-5)
DDPM	3.0e-2 (2.4e-3,6.8e-2)	1.7e-1 (2.3e-2,9.e-1)	1.2e-2 (2.4e-3,2.9e-2)	9.7e-3 (3.5e-3,2.1e-2)	1.3e-5 (0.e+0,4.1e-5)
NCSN	7.3e-1 (7.7e-3,2.9e+0)	3.e+0 (4.1e-2,1.8e+1)	2.7e-1 (2.1e-3,1.2e+0)	4.2e-1 (9.e-3,2.8e+0)	1.2e-5 (7.e-6,2.4e-5)
GANO	1.9e-1 (6.3e-2,5.7e-1)	8.3e+0 (1.5e+0,1.7e+1)	4.1e-2 (1.1e-2,1.1e-1)	3.2e-1 (5.8e-2,8.2e-1)	6.2e-4 (3.1e-5,2.2e-3)

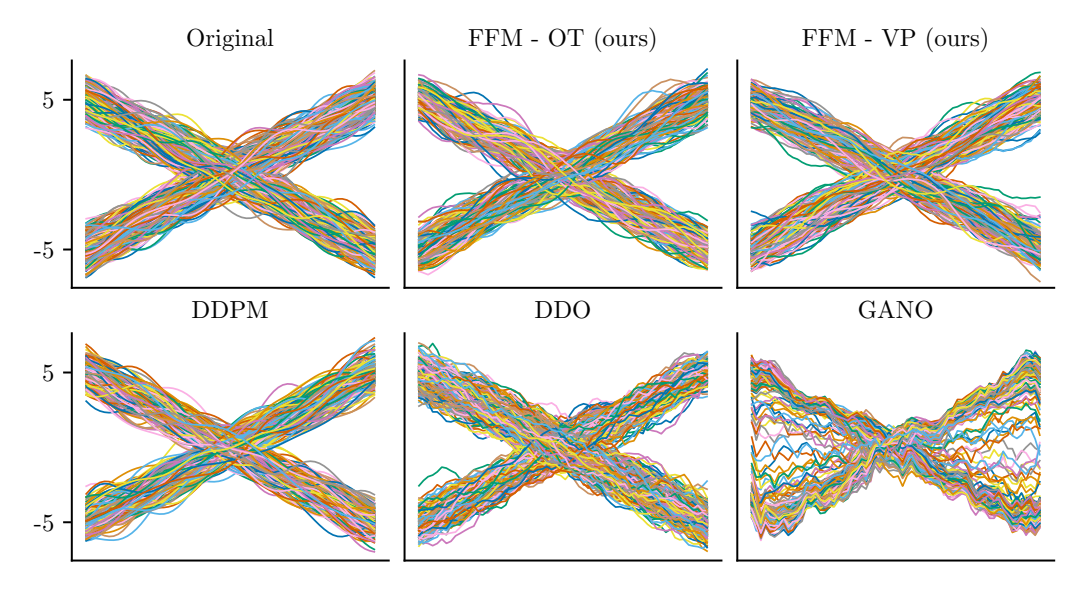


Figure 4: Unconditional generation of 500 samples from various models trained on the synthetic MoGP dataset. Samples from our FFM model and DDPM appear visually to better match the characteristics of the real data (top left) relative to DDO and GANO. See Table 3 for a quantitative comparison.

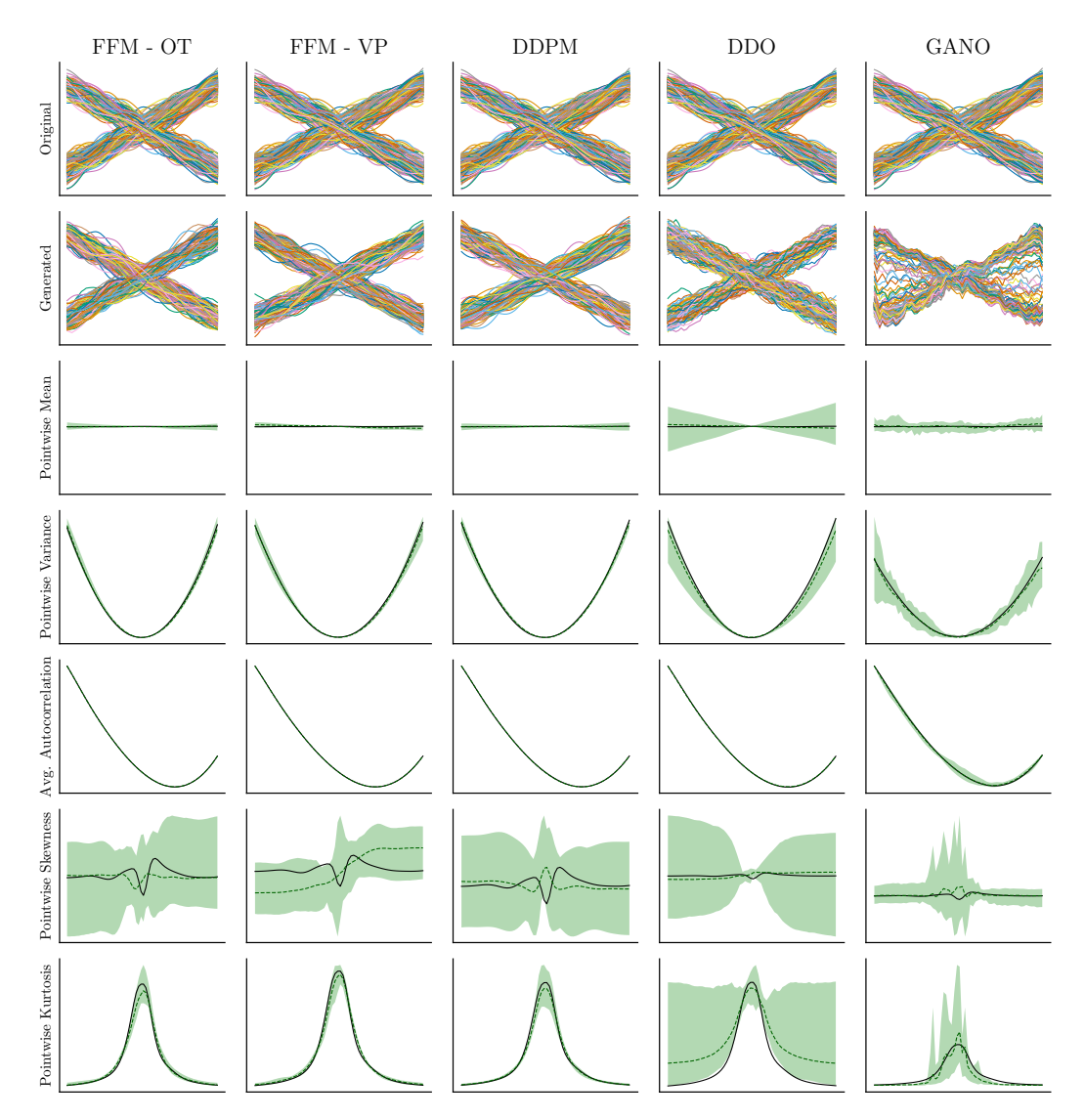


Figure 5: Various pointwise statistics on the MoGP dataset. Curves in black indicate the corresponding pointwise statistic for the original dataset (top row). The green error bands represent the minimal and maximal value of the pointwise statistic from 500 samples across ten random seeds of the corresponding model. The dashed green lines indicate the mean pointwise statistic across these ten runs for each model. See Table 3 for a quantitative comparison.

# A.3.2 Additional Results: AEMET

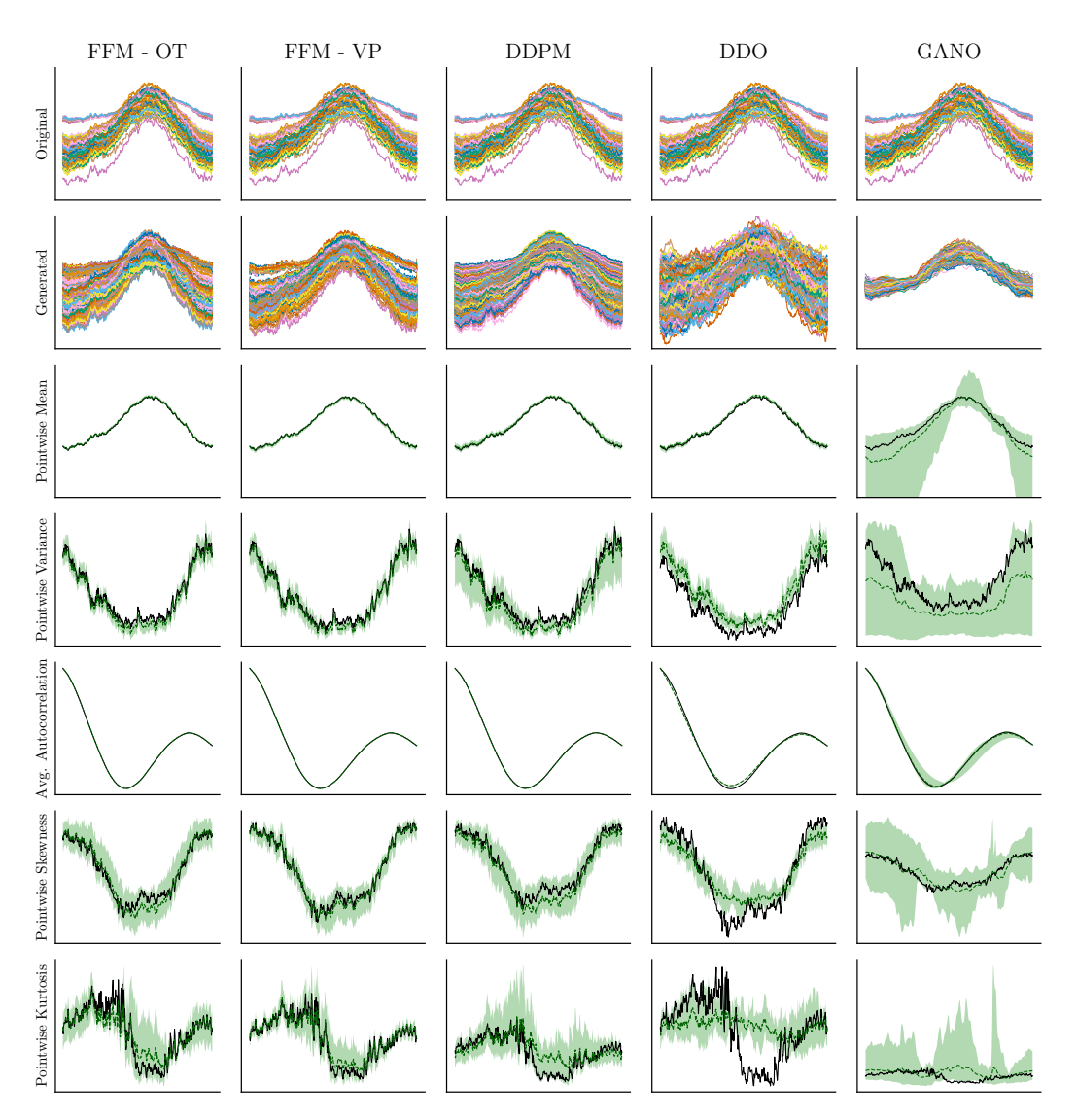


Figure 6: Various pointwise statistics on the AEMET dataset. Curves in black indicate the corresponding pointwise statistic for the original dataset (top row). The green error bands represent the minimal and maximal value of the pointwise statistic from 500 samples across ten random seeds of the corresponding model. The dashed green lines indicate the mean pointwise statistic across these ten runs for each model. See Table 1 for a quantitative comparison.